High-capacity ion trap coupled to a time-of-flight mass spectrometer for comprehensive linked scans with no scanning losses

Sunnie Myung, Herbert Cohen, David Fenyö, Julio C. Padovan, Andrew N. Krutchinsky, Brian T. Chait *

The Rockefeller University, New York, NY, USA

ARTICLE INFO

ABSTRACT

A high-capacity ion trap coupled to a time-of-flight (TOF) mass spectrometer has been developed to carry out comprehensive linked scan analysis of all stored ions in the ion trap. The approach involves a novel tapered geometry high-capacity ion trap that can store more than 10^6 ions (range 800–4000 m/z) without degrading its performance. Ions are stored and scanned out from the high-capacity ion trap as a function of m/z, collisionally fragmented and analyzed by TOF. Accurate mass analysis is achieved on both the precursor and fragment ions of all species ejected from the ion trap. We demonstrate the approach for comprehensive linked-scan identification of phosphopeptides in mixtures with their corresponding unphosphorylated peptides.

© 2010 Elsevier B.V. All rights reserved.

1. Introduction

The development of effective ionization methods for analyzing peptides and proteins (i.e., matrix-assisted laser desorption ionization (MALDI) [1] and electrospray ionization [2]) has made mass spectrometry (MS) an invaluable tool for proteomic research [3]. Even though extremely effective mass spectrometric configurations have been developed for analyzing increasingly complex proteomic samples (see e.g., [4,5]), it is still not possible to extract comprehensive information from the samples of interest. Difficulties arise because the samples often contain thousands of proteolytic fragments, which are present in a wide range of abundances, and the components of greatest interest are frequently those that are less abundant. In addition, the information must often be acquired on a time-scale commensurate with the rapid elution times of peptides from chromatographic separations. Adding to the analytical challenge is the desirability of extracting several different types of information from the sample, including the accurate molecular masses of the peptides, backbone fragmentation information, the presence and locations of posttranslational modifications, and particular fragmentation transitions that identify and quantitate proteins of interest or their modifications (so-called multiple reaction monitoring (MRM) or hypothesis-driven mass spectrometry) [6].

One technique that has proved to be particularly successful for proteomic studies is data-dependent tandem mass spectrometry (data-dependent MS/MS) (see e.g., [7,8]). In this strategy, mass spectra of eluting chromatographic fractions are obtained, rapidly analyzed in real time, and the resulting information is used to direct isolation and MS/MS of the detected peptide ions. The real challenge in this approach is to obtain the information with sufficient sensitivity before the fractions of interest have finished eluting. Here, the first step is the collection of a single stage mass spectrum, followed by a sequential series of tandem mass spectra directed by information obtained in the first step. Because the strategy follows this repeating multistep sequence, the process is inherently inefficient with the efficiency decreasing in proportion to the length of time needed to collect the single stage mass spectrum and the number of data dependent tandem mass spectra collected per unit time. This inefficiency can be ameliorated in cases where the peptides of interest and their characteristic fragmentation transitions are postulated prior to the experiment, as in MRM [6]. However, the MRM approach (i) is highly focused on known protein actors and assumes that unexpected proteins can be neglected in the biological process under study; (ii) it involves considerable front-end work on standard peptides, and (iii) it requires that interferences occurring in the expected transitions be detected and corrected for. In special cases, where it is desired to monitor a single type of transition, as for example in the detection of phosphopeptides via neutral loss of the elements of phosphoric acid (H_3PO_4) (reviewed in [9]), it is not necessary to first collect a single-stage mass spectrum. Rather, such transitions can be specifically observed without prior knowl-

---

* Corresponding author.
  E-mail address: chait@rockefeller.edu (B.T. Chait).

edge of the precursor peptide masses, in the so-called "linked-scan neutral loss experiment", which are typically performed on triple quadrupole or related types of mass analyzers [10–13]. By the use of appropriate instrumentation, such as the quadrupole/time-of-flight (QTOF), it proves feasible to generalize this experiment to analyze many transitions in parallel [14,15]. While such linked-scan experiments are highly useful for detecting specific transitions and therefore specific peptide modifications, this approach suffers from "scanning losses". The loss in efficiency that arises from these scanning losses is given by $\Delta M/M$, where ΔM is the mass window that is scanned across the mass range of interest, M. Typical efficiencies for such linked-scan experiments are ~0.001.

A number of strategies have been explored in attempts to overcome such efficiency losses in tandem mass spectrometric experiments. These include multiplexed TOF MS/MS [16–23], multiplexed ion trap MS/MS [24], multiplexed tandem FTICR by selecting several peptides for simultaneous dissociation [25–27], or the combination of storage and ion mobility devices with TOF MS [28–32]. In the present work, we explore a new strategy wherein ions produced in an ion source are first trapped in a high-capacity ion trap, after which they are sequentially ejected as a function of m/z, fragmented and analyzed by orthogonal injection TOF-MS. A typical time sequence for this approach involves storage of ions for 1 s followed by fragmentation and analysis for 1 s, and repetition of this sequence for as long as is desired. The degree of fragmentation is tuned to leave a fraction of each of the precursor ion species intact, so that both precursor and fragment ions can be measured for each ejected species at the full resolution and accuracy of the TOF analyzer. In this way, all ion species that are stored in the ion trap are analyzed without scanning losses. The key aspect of this approach is that there is no need to introduce data-dependent strategies since the entire collection of trapped ion species is analyzed. Rather, any particular type of information that resides in this comprehensive data set (e.g., parent ion masses, backbone fragmentation, neutral losses, MRM transitions etc.) can be extracted by a computer algorithm after data acquisition is complete, thus providing a comprehensive set of information for any particular sample.

2. Experimental

2.1. High-capacity ion trap "Qtap"

The high-capacity tapered geometry ion trap ("Qtap") used in this work has been discussed in detail previously [33]. Hence, only a brief description will be provided here. As shown in Fig. 1, the ion trap consists of eight tapered rods held together by a small central linear ion trap (length 10 mm). The Qtap is filled with helium to a pressure estimated to be 5 mTorr. The whole ion trap is 31.4 cm long and the diameter of each tapered rod (length 152 mm) changes linearly from 7.21 mm to 10.4 mm. In the middle of the linear ion trap is a slit (7.6 mm × 1 mm) through which stored ions are ejected. The ion trap is driven by an independent RF power supply (RF frequency 333 kHz) and a secondary, low-voltage resonance ejection RF that is set at 265 kHz. These frequency values were found empirically based on the optimal combination of resolution, sensitivity, and the m/z range of the ion trap [33]. The secondary RF is only applied to one pair of rods as shown in Fig. 1. The purpose of the tapered geometry is to create an electric potential that closely approximates a linear quadrupole at any point along its z axis, with the field radius scaling as a function of position on the z axis as previously described [33]. This geometry results in an effective potential well, with steeper walls at the ends of the trap, and shallower well towards the center, thus forcing the ions towards the center of the trap when the RF voltages are ramped. Initially during the fill time,
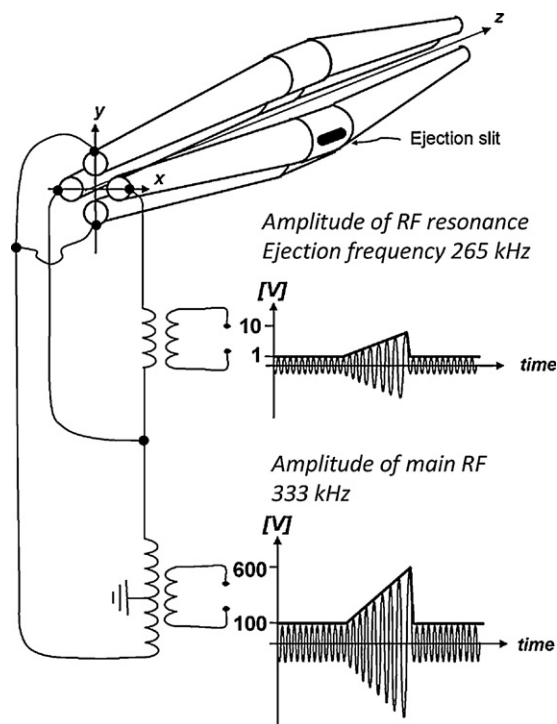

Fig. 1. Schematic diagram of the high-capacity ion trap "Qtap" using tapered geometry rods. The frequencies of the main RF and excitation RF are 333 and 265 kHz, respectively.

the amplitude of the main RF voltage is maintained at 100 V and the secondary resonance ejection RF at 2 V for a specified time period, usually 1 s. During this time the injected ions are stored about the central axis of the trap. After the fill time, the main and ejection RF amplitudes are ramped over a period of 1 s to 600 V and 6 V, respectively. These time-varying potentials cause ions to be ejected sequentially as a function of mass through a slit in one of the connecting quadrupole rods [33]. During the ejection process, lighter ions at the ends of the trap are swept towards the center first. Under these conditions, ions will oscillate in the y-axis, which will in turn increase the motion of the ions towards the z axis-driving the ions towards the center of the trap. During this process the larger ions will remain unaffected and will only be excited when sufficiently high amplitude RF is applied. In this manner, ions are sequentially compressed towards the center of the trap, according to their m/z value, where they are eventually ejected through a small slit made in one of the rods.

2.2. Ion source and laser system

The compact disc ion source has been described in detail previously [34]. Briefly, ions are produced by short duration (4 ns) pulses of 337 nm wavelength laser light (nitrogen laser, VSL-337, Spectra Physics, Mountain View, CA) operating at a repetition rate of 10–20 Hz. The beam is reflected by a mirror, passed through a lens (f = 10 cm) and then through a quartz window, reaching the surface of the compact disc at an angle of incidence of 60°. The dimension of the short axis of the elliptical laser spot on the sample surface is 0.3–0.5 mm. When using the MALDI matrix 2,5-dihydroxybenzoic acid (DHB), we use a laser power density on the spot of ~$(1-5) \times 10^7$ W/cm^2. When using the matrix 4-chloro-α-cyanocinnamic (4ClCCA) [35], we reduced the power density of the laser by changing the distance of the lens to the target spot (i.e., the spot size). The laser spots were monitored by a video camera.

2.3. Configuration I: Qtap-qTOF

In order to induce fragmentation of ions ejected from the Qtap and to measure the resulting fragment and residual precursor ions, we coupled the Qtap to a quadrupole orthogonal geometry TOF MS (Fig. 2a). Experiments with this configuration were carried out as follows: ions produced in a MALDI source were introduced into a quadrupole ion guide filled with helium ($\approx 2 \times 10^2$ Torr), guided into the Qtap (pumped with a 250 L/s turbo pump (Turbo V-250 Varian)), stored for 1 second and then scanned out for 1 s. This timescale was used because it takes a minimum of 1 ms to fragment an ejected packet of ions, cool these fragments, and pulse them into a mass analyzer without interference from previously ejected ions (i.e., to avoid crosstalk). Thus if it takes 1 ms per ~ 3–$4 m/z$ units, we need ~ 1 s to perform MS/MS experiment over a range of 4000 m/z. This gives us a duty cycle of 50% [33]. Upon ejection, ions were focused into a quadrupole collision cell filled with argon at a few millitorrs. The quadrupole consists of rods that are 9 mm in diameter and 213 mm length and is pumped by a separate 250 L/s turbo pump (Turbo V-250 Varian). The collision cell is a quadrupole with a "LINAC" accelerator set at 100 V to assist in the rapid extraction of precursor and fragment ions from the collision cell. Upon exiting the collision cell, ions were focused into a reflectron geometry TOF mass spectrometer (Sciex, Centaur prototype [36]), pumped by a 550 L/s turbo pump (Turbo V-550 Varian). Here, voltage pulses sup-

plied at 5000 Hz were used to initiate the TOF scans. The TOF scan times ($\approx 200 \mu$s duration) are much shorter than the Qtap ejection times for each sequential m/z from the Qtap (a few milliseconds duration). Thus the TOF analyzer can provide rapid analysis of all the ions from the ion trap with high mass resolution.

Limitations of the Qtap-q-TOF: this simple configuration has two main limitations. First, due to the lack of an intermediate cooling/collimating quadrupole, it is not possible to optimally change the energies of the ions as a function of m/z when they are ejected from the Qtap into the collision cell. Rather, these energies are largely set by the corresponding effective potential well determined by the amplitude of the main RF voltage and, to a lesser extent, by the helium pressure within the Qtap. Despite this lack of control over the energies of the ions, we were able to obtain neutral losses by increasing the excitation amplitude potential of the Qtap and tuning the amount of argon in the collision cell. The second limitation results from the insufficient gas isolation between the argon-filled collision cell and the helium-filled Qtap. Since argon contamination of the Qtap severely compromises its performance, it was necessary to limit the argon pressure in the collision cell to reduce gas crosstalk between the collision cell (7 mm × 3 mm aperture) and the Qtap cell (7.5 mm × 4.8 mm aperture). Helium pressure in the Qtap and argon pressure in the quadrupole were carefully controlled with capillary restriction tubes connected to pressure regulators [37].
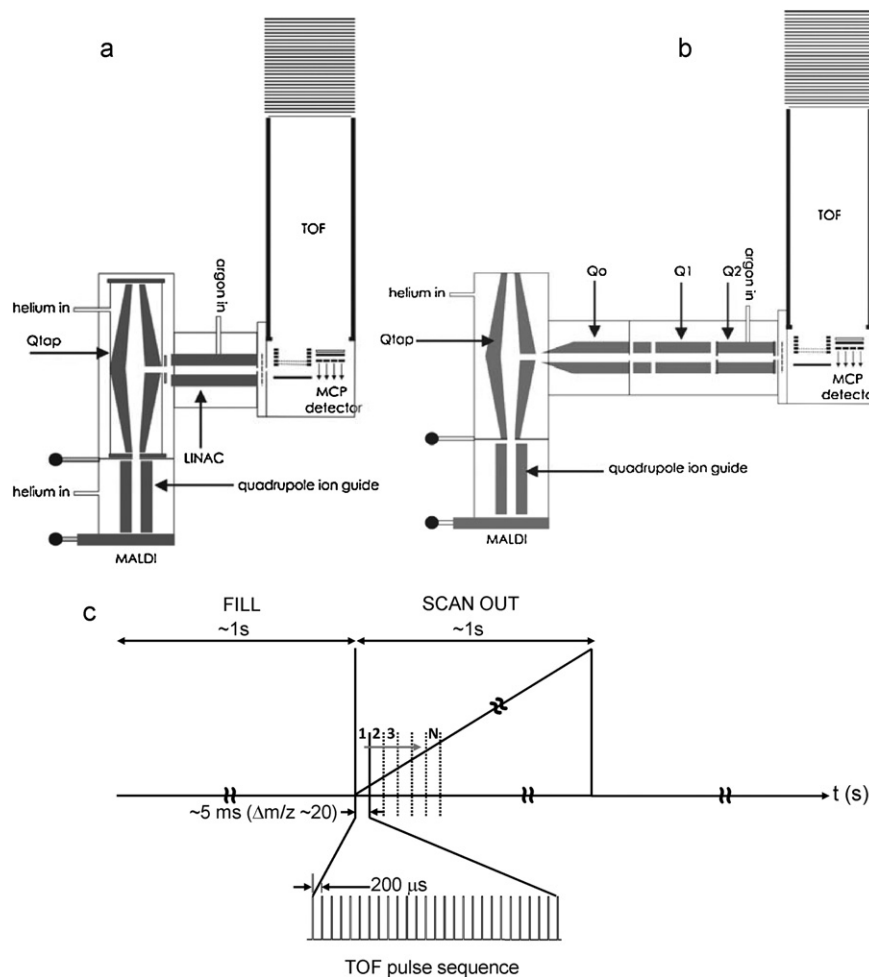

Fig. 2. (a) Schematic of the compact Qtap-qTOF instrument. A LINAC collision cell and an orthogonal TOF are situated right after Qtap. (b) Schematic of the extended Qtap-qQq-TOF instrument. This configuration is similar to the compact version except there are two additional quadrupoles (Qo and Q1) before the collision cell. (c) The pulse sequence for the one full cycle of fill and scan out time for Qtap and the bottom shows the TOF pulse sequence corresponding to ≈5 ms window in Qtap dimension. TOF is pulsed at 5 kHz (200 us).

2.4. Configuration II: QTAP-qQq-TOF

The second configuration (Fig. 2b) is an extended version of the compact Qtap-q-TOF shown in Fig. 2a. This setup allows for better control of the energies of the ions and the pressure in each region because the Qtap is decoupled from the collision cell by extra quadrupoles (Q_o and Q_1) thus preventing argon contamination of the Qtap. In addition, the fragmentation energy as a function of m/z is tunable by changing the potential difference between Q_o and the entrance lens of the collision cell. Because the energy required for the ions are proportional to the m/z values, the Q_o potential was modulated by syncing the DC potential of Q_o to the Qtap ejection scan. The Q_o potential was ramped from 40 to 150 V for a peptide mixture with m/z ranging from 500 to 4000.

In this configuration, MALDI-generated ions were also stored for 1 s and then scanned out of the Qtap over a period of 1 s. Upon ejection from the ion trap, ions were focused and cooled in the RF-only Q_o and Q_1 ion guides before being accelerated into Q_2 for fragmentation. It is important to note that Q_1 here is used in RF only mode and not as a resolving mass analyzer. The quadrupole collision cell Q_2 was filled with argon gas to an estimated pressure of several millitorr. The degree of fragmentation in Q_2 was tuned to leave a portion of the precursor ion unfragmented, whereupon both the fragment ions and remaining precursor ions were analyzed by TOF with high mass resolution. This approach allows us to obtain comprehensive MS/MS analysis of all ejected ions.

2.5. Pulse sequence and data analysis

A critical feature of the interface between the Qtap and the TOF analyzer is the timescales of the experiment. The Qtap (fill time ≈1 s), and subsequent ejection/collisional dissociation (a few milliseconds per m/z unit), allow for the use of TOF analysis (200 μs/spectrum) for the measurement of all precursor and fragment ions with high mass accuracy. Fig. 2c shows the pulse sequence for the storage and ejection process for the Qtap followed by TOF analysis. Ions are injected and stored for 1 s, then sequentially scanned out of the Qtap in 1 s, and pulsed into a flight tube at 5 kHz.

Flight times were acquired using a four-channel time-to-digital converter (TDCx4, IonWerks, Houston, Texas) from a 4-anode detector [38,39], and recorded on a Macintosh computer using the "TOFMA" data acquisition software (TOF laboratory, University of Manitoba, Canada). Data was saved event-by-event, with records of both the Qtap ejection time and the TOF for every ion that hit the detector. The data were analyzed post-acquisition using in-house software that allows us to bin the data by integrating regions of the Qtap ejection time window. The size of the integration window was matched to the resolution of the Qtap – usually a 5 ms window size was used (i.e., 200 regions covering the 1s ejection time spectrum). Once the dataset was recorded and binned, the Qtap ejection time was calibrated to the precursor ion m/z. This process is computationally straightforward because we intentionally leave a significant portion of the precursor ions intact. Subsequently, all precursor ion masses were determined with high accuracy (<10 ppm) by measuring the centroid of peaks in the TOF spectrum precursor ion isotope cluster. The calibration allows us to find the precursor ion m/z within any 5 ms Qtap ejection time window. Neutral loss scans were extracted by integrating the regions of the TOF spectra that corresponded to the expected neutral loss. These neutral-loss intensities were plotted as a function of Qtap ejection time. We note that both precursor and fragment ions were determined with high mass accuracy, so that integration of the neutral loss intensities could be done separately for each isotopic peak, thus yielding high signal-to-noise ratios.

2.6. Sample preparation

The experiments presented here used a combination of the following samples: (1) standard mixture of unphosphorylated peptides: bradykinin fragment 2–9 (903.46 Da, PPGFSPFR), substance P (1346.7 Da, RPKPQQFFGLM-NH$_2$), neurotensin (1671.9 Da, pELYENKPRRPYIL), amyloid β-protein fragment 12–28 (1954.0 Da, VHHQKLVFFAEDVGSNK) or ACTH fragment 1–16 (1935.9 Da, SYSMEHFRWGKPVGKK), ACTH fragment 1–24 (2931.6 Da, SYSMEHFRWGKPVGKKRRPVKVYP), and oxidized insulin β-chain from bovine insulin (3493.6 Da, FVNQHLC(SO$_3$H)GSHLVEALYLVC(SO$_3$H)GERGFFYTPKA); (2) phosphorylated peptides: [pS^{119}]CREB327 fragment 113–123 (1467.8 Da, ILSRRPpSYRKI), PKA inhibitor substrate (1573.8 Da, GRTGRRNpSIHDIL), aquaporin-2 fragment 254–267 (1712.8 Da, RQSVELHpSPQSLPR), and AKT/PKB/Rac-protein kinase substrate (1794.8 Da, ARKRERTYpSFGHHA) and one glycosylated peptide ([GalNAc-Ser] erythropoietin fragment 117–131 (1667.8 Da, EAISPPDAA(GalNac)SAAPLR); (3) a mixture of peptides obtained from tryptic digestion of ovalbumin (Sigma, St. Louis, MO). All standard unphosphorylated peptides were obtained from Sigma (St. Louis, MO) and phosphopeptides were from Anaspec (Fremont, CA).

Matrix: fresh, saturated solutions of 2,5-dihydroxybenzoic acid, (DHB, MW = 154.1 Da, Sigma) and 4-chloro-α-cyanocinnamic acid (4ClCCA, MW = 207.6, Key Organics Ltd., UK) were prepared in 70% acetonitrile/0.1% TFA (v/v) just prior to measurements. To prepare DHB samples, a volume of a stock solution (1 pmol/μl per component) was diluted by half with an equal volume of the saturated DHB solution and 2 μl of the resulting solution were spotted on the CD sample plate. To prepare for 4ClCCA samples, a stock solution was diluted 10 times with 25% saturated matrix solution to obtain a final concentration of 100 fmol/μl per component in 70% acetonitrile/0.1%TFA (v/v) and 2 μl of the resulting solution were spotted on the CD plate.

Ovalbumin tryptic peptides: A mixture of tryptic peptides were prepared from 36 μM of ovalbumin (Chicken egg white, Grade VII, Sigma, St. Louis, MO) dissolved in 100 mM ammonium bicarbonate solution. To reduce the disulfide bonds the solution of proteins was treated for 1 h at 57 °C with 20 mM dithiothreitol (DTT). The subsequent S–H bonds were alkylated by adding 50 mM of iodoacetamide (in the dark at room temperature for 45 min). The reduced and alkylated proteins were then digested with sequencing grade trypsin (Promega) at a trypsin:protein ratio of 1:40 (w:w) overnight at room temperature. The resulting stock solution (10 pmol/μl) was diluted with 70% acetonitrile/0.1% TFA just prior to measurement and used for MALDI analysis.

3. Results

3.1. Qtap peak resolution

To evaluate the peak widths of individual ion species that are ejected from the Qtap as a function of m/z, we recorded the ejection time distribution of several peptide ion species (Fig. 3) using the compact version of the instrument (Fig. 2a). In the portion of the time spectrum (m/z) shown, three ion species at m/z values of 1347.736, 1672.918, and 1955.014 are observed at t_{Qtap} of 0.07, 0.17, and 0.24 s, respectively. In this setup, ions are scanned out of the Qtap filled with ≈5 mTorr of helium into a collision cell filled with a few millitorrs of argon, before being pulsed into an orthogonal TOF. The FWHM of the peaks was ≈5 ms (Fig. 3), providing an effective resolution of ≈200, which corresponds to peak widths of 10–20 Da FWHM. To test whether collisional damping by argon in the collision cell contributes to this width, we used a LINAC collision cell [39], wherein the precursor and fragment ions are accelerated
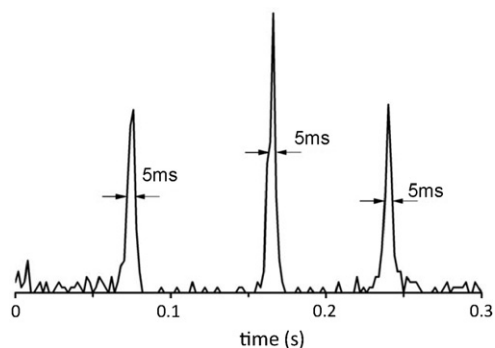
Fig. 3. MALDI Qtap ejection time (mass) spectrum obtained from a 5 peptide mixture (500 fmol of each component) measured in a single 1-s scan using the Qtap-qTOF instrument. Only a narrow region is shown for 3 out of the 5 peptides. Each of the peaks has FWHM ≈5 ms.

through the collision gas. Such acceleration did not appreciably reduce the peak widths of the ejected ions.

3.2. Qtap-qTOF single-stage MS measurements of a peptide mixture

Fig. 4 (2nd from top panel) shows the time-resolved (i.e., mass-resolved) Qtap ejection distribution of a five-peptide mix-
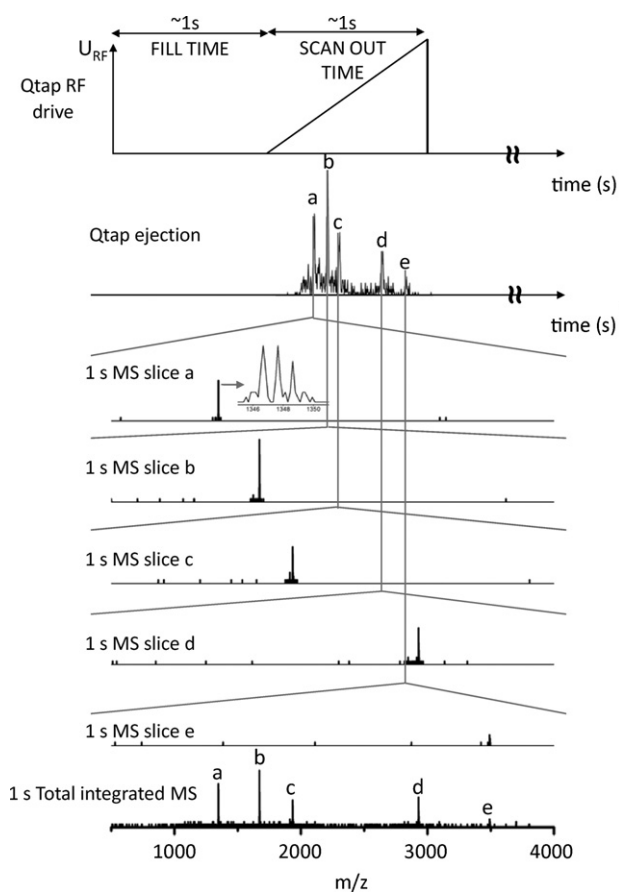

Fig. 4. (Top) Schematic diagram of Qtap RF drive timing and (2nd from top) MALDI Qtap ejection time (mass) spectrum obtained by filling the Qtap for a period of 1s and then scanning the ions out of the Qtap over a period of 1 s. The dataset was obtained from a 5 peptide mixture (100 fmol of each component). (Bottom) Individual TOF mass spectra obtained by integrating the TOF spectra over a narrow time region about the solid gray line shown in the Qtap ejection time spectrum. The inset provides an expansion of the TOF spectrum of peak a, showing the isotopic distribution with a resolution of ≈6000 FWHM. The bottom spectrum corresponds to the total integrated TOF spectrum obtained in 1 s.

ture (100 fmol of each component) obtained in a single 1-s scan from the Qtap-qTOF instrument (Fig. 2a). The MALDI generated ions are cooled by collisions with helium gas in the post-ion source quadrupole ion guide and then enter the Qtap, operating in the fill mode where the amplitude of the main RF and the secondary resonance ejection RF is 100 V and 2 V, respectively. Subsequent to the 1-s fill, ions are scanned out by ramping the amplitudes of the main and secondary resonance ejection RF voltages at rates of ≈500 V/s and ≈5 V/s, respectively. This scan results in ions being ejected from the Qtap from low to high m/z values. The ejected ions enter the quadrupole collision cell (filled with helium gas for cooling so that no fragmentation occurs), which acts in this case as a simple ion guide. The cooled and collimated ions are guided into an orthogonal geometry TOF for mass measurement. The middle five panels show the TOF MS obtained by integrating the data from narrow time slices ($\Delta t = 10$–20 ms) about each of the five peaks (a–e), providing mass spectra for each peptide ion species ejected from the Qtap. The full TOF mass spectrum obtained by integrating the data across the whole ejection scan is shown at the bottom of Fig. 4. Despite the modest Qtap resolution ($R_{FWHM} \approx 200$), the peptide masses are measured in the TOF analyzer at its full mass resolution ($R_{FWHM} \approx 6000$), as shown by the isotopic distribution of the first peptide peak in the inset of Fig. 4.

3.3. Utility of Qtap-qTOF as a linked-scan instrument

The linked scan technique is useful for detecting the presence of post-translational modifications (e.g., phosphorylation) via detection of the loss of the elements of phosphoric acid (H_3PO_4, – 97.976 Da) [40,41]. This technique is often implemented in triple quadrupole mass analyzers, where the first and the last quadrupoles are scanned in synchrony to detect the loss of a specific neutral fragment. In the present Qtap-qTOF instrument, we perform such neutral loss analyses using a computer algorithm that we implement subsequent to data acquisition (see Section 2.5). Because all ions ejected from the Qtap and fragmented are analyzed, a major benefit of this approach is to eliminate the need for scanning a small window of ions through the quadrupoles, and hence eliminate the loss of efficiency due to the ion selection/rejection steps involved in scanning. For this experiment, we used the setup shown in Fig. 2a with a few millitorrs of argon in the collision cell to induce dissociation and dampening of ion motion prior to their injection into the TOF analyzer. Here, all ejected ions are subjected to fragmentation with no precursor ion selection and subsequently all the resulting fragment ions and remaining precursor ions are detected in the TOF analyzer. The translational energy gained by ions during the ejection process [33] yielded sufficiently energetic collisions with the argon atoms in the collision cell to induce loss of H_3PO_4 (∼98 Da) from the phosphopeptides. In the case shown, we analyzed a mixture containing 6 unphosphorylated, 4 phosphorylated, and 1 glycosylated peptides (250 fmol of each component) introduced from the MALDI ion source. The top panel of Fig. 5a shows the Qtap ejection time (mass) spectrum of this mixture. The most intense peaks arise from the unphosphorylated peptide components. Shown in the next panels are TOF spectra of Qtap ejection time slices labeled a–d, which show the phosphopeptide precursors together with signature losses of 98 Da. To obtain the equivalent H_3PO_4 neutral loss linked-scan spectrum, the intensities of neutral losses of 97.976 Da for all the spectra were plotted as a function of Qtap ejection time (see Section 2.5). As shown in Fig. 5b (middle panel), this procedure allows us to readily extract the signature 97.976 Da neutral loss peaks for all the phosphopeptides in the mixture. In a similar manner, we were able to detect the presence of the single glycopeptide by detecting its GalNac signature loss of 203.079 Da (Fig. 5b, bottom panel). Although the glycosylated peptide was not resolved from an unphosphorylated peptide in the
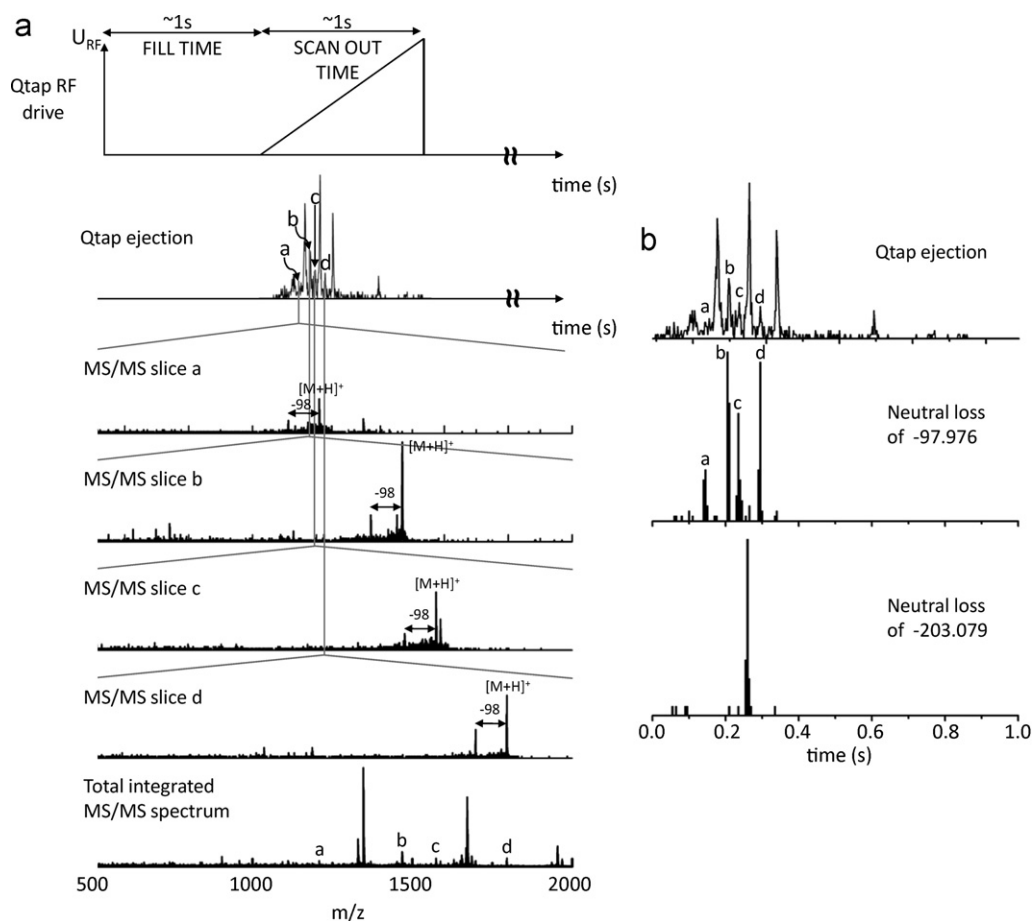
Fig. 5. (a) (Top) Schematic diagram of Qtap RF drive timing and (2nd from top) Qtap ejection time (mass) spectrum of MALDI ions from a peptide mixture containing unmodified, phosphorylated, and glycosylated peptides (250 fmol of each component). (Middle) Individual MS/MS spectrum obtained by integrating a narrow region along the gray solid line shown in the Qtap ejection time spectrum. Each of the MS/MS spectra corresponds to one of the four phosphopeptides in the mixture with the characteristic loss of 98 Da from the phosphoric acid. (Bottom) Total integrated MS/MS TOF spectrum. (b) (Top) Qtap ejection time (mass) spectrum for the peptide mixture. (Middle) Neutral loss of 98 Da (phosphoric acid elimination) for the four phosphopeptides in the mixture, extracted post-data acquisition. (Bottom) Neutral loss of 203 Da for the single GalNac peptide in the mixture, extracted post-data acquisition.

Qtap time spectrum (because their masses are only 2 Da apart), only the glycosylated peptide was picked in our post-collection linked-scan analysis because only the glycosylated precursor ion loses precisely 203.079 Da. This experiment illustrates how the present Qtap-qTOF instrument can be utilized as a versatile detection system for specific neutral loss detection that yields data equivalent to that obtained from linked scan experiments. In addition, because all the analysis is carried out post-data acquisition, no data-dependent acquisition is required and no prior knowledge of which modifications are present in the sample is needed.

3.4. Dynamic range measurements

We tested the dynamic range of the Qtap-qTOF instrument by taking MALDI spectra of a 4 peptide mixture (250 fmol of each peptide) spiked with a single phosphopeptide at various concentrations. The spiked phosphopeptide is indicated by the arrow in the Qtap time (mass) spectrum shown in Fig. 6a (left panel). Three representative Qtap ejection time (mass) spectra are shown: 250 fmol of unphosphorylated peptides with 250 fmol, 100 fmol, and 25 fmol of the single phosphopeptide. The dominant peaks in each of the Qtap ejection time (mass) spectra correspond to unphosphorylated peptides. The right hand panels of Fig. 6a show the H_3PO_4 neutral loss linked-scan spectra from these three spiked samples, showing that we can readily detect by our post-data acquisition neutral loss

scan analysis 25 fmol of phosphopeptide spiked into 250 fmol of unphosphorylated peptides.

3.5. Detecting a phosphopeptide in a proteolytic digest

We also performed our post-data acquisition neutral loss scan analysis on a tryptic digest of the well studied phosphoprotein, chicken egg white ovalbumin. The majority of the ions in the total integrated mass spectrum correspond to unphosphorylated peptides from ovalbumin (Fig. 6b, top left), with only a single phosphopeptide present in this preparation (indicated by the star). By extracting the narrow region of the Qtap ejection time (mass) spectrum indicated with the star (Fig. 6b, top right), only the phosphopeptide MS/MS spectrum was obtained. Despite the obviously inefficient fragmentation in this particular case (Fig. 6b, bottom left), we were able to detect the loss of 97.976 Da from the phosphorylated precursor peptide FDKLPGFGDpSIEAQCGTSVNVHSSLR as shown with the neutral loss scan in the bottom right hand panel of Fig. 6b.

3.6. Qtap-qQq-TOF configuration

We also tested out the properties of the more extended Qtap-qQq-TOF configuration shown in Fig. 2b. To do this, we simply coupled the Qtap to an existing qQq-TOF mass analyzer (Sciex,
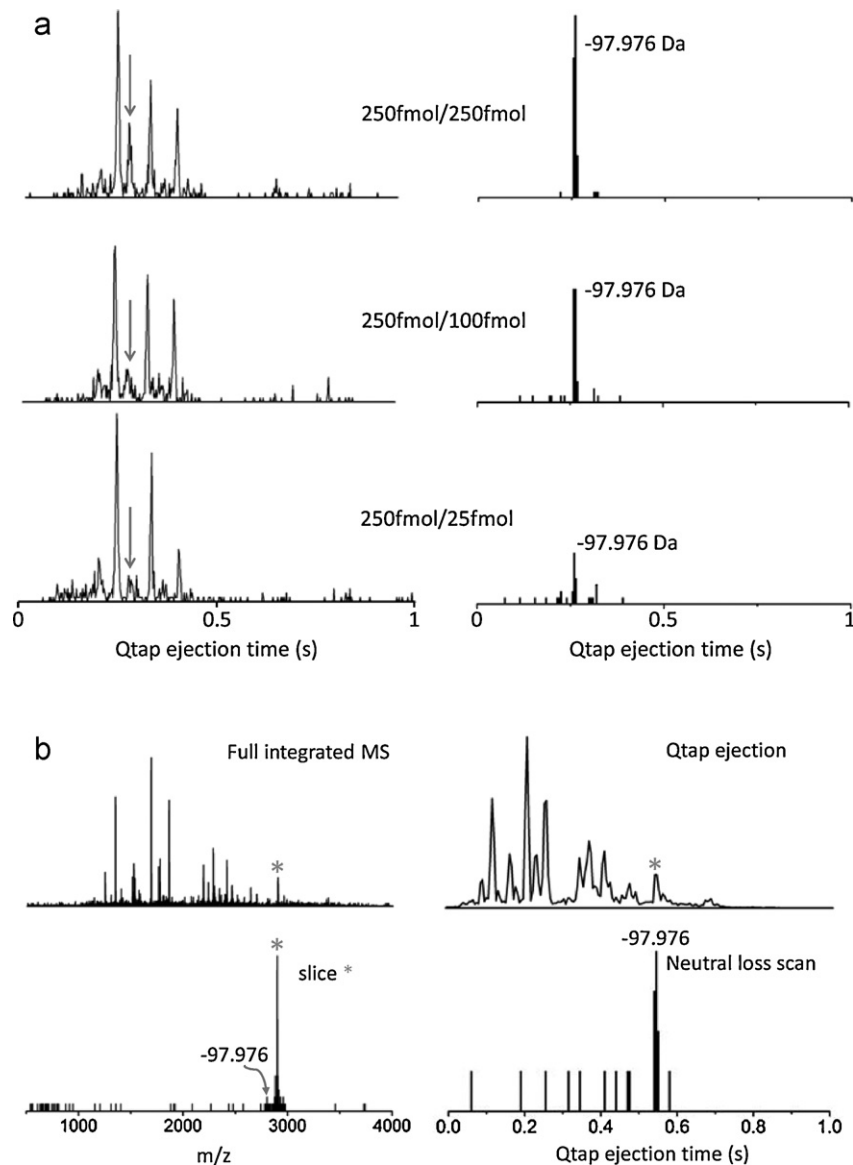
Fig. 6. (a) Left, shows the Qtap ejection time (mass) spectrum of a mixture of peptides (250 fmol of each component) containing four unmodified peptides: Bradykinin fragment 2–9 [m/z 904.468, PPGFSPFR], Substance P [m/z 1347.737, RPKPQQFFGLM-NH2], neurotensin [m/z 1672.916, pELYENKPRRPYIL], and ACTH fragment 1–16 [m/z 1936.985, SYSMEHFRWGKPVGKK] mixed with a single phosphopeptide ([pS119]CREB327 fragment 113–123 [m/z 1468.823, ILSRRPpSYRKI]) at 250 fmol, 100 fmol, and 25 fmol concentrations. Right, shows the neutral loss of 98 Da Qtap ejection time (mass) spectra obtained for each dataset shown to the left. See text for more detail. (b) Left, top is the full integrated mass spectrum obtained from a 250 fmol ovalbumin digest. The majority of the ions in the spectrum correspond to unphosphorylated peptides, with the single phosphopeptide (m/z 2901.247, FDKLPGFGDpSIEAQCGTSVNVHSSLR) in the mixture indicated by a star. Left, bottom is the individual TOF MS/MS spectrum obtained for the phosphopeptide by integrating a narrow region in the Qtap time spectrum during which the phosphopeptide is ejected. Right, top shows the total Qtap ejection time (mass) spectrum from the ovalbumin digest with the single phosphopeptide in the mixture indicated by a star. Right, bottom shows the corresponding neutral loss of 98 Da Qtap ejection time (mass) spectrum. As expected, only one phosphopeptide is detected in the mixture.

Centaur prototype). In contrast to the Qtap-qTOF configuration (Fig. 2a), in this second configuration (Fig. 2b) the helium-filled Qtap is decoupled with respect to gas exchange from the argon-filled quadrupole collision cell. This is advantageous because argon contamination of the helium in the Qtap adversely affects its performance (data not shown). In 3-D ion traps such adverse performance due to heavy impurity gases within the helium buffer gas has previously been attributed to the increase in ion scattering [42]. As a result, commercial 3-D and linear ion traps are well isolated from heavy gas contamination by the incorporation of efficient differential pumping and ion guides. Furthermore, this extended configuration allows us to better control the energies of the ions entering the collision cell – in this case determined by the potential difference between Q_o and the entrance lens of the collision cell, Q_2 (Fig. 2b). Fig. 7(top) shows a Qtap ejection time (mass) spectrum for a 5 peptide mixture obtained with this configuration. We have found previously that the collision energy for optimal fragmentation scales linearly with m/z [43]. Therefore, the collision energy was varied in proportion to the m/z of the ejected ions by ramping the potential on Q_o, from 40 to 100 V, in sync with the Qtap RF scan. At the same time, the collision energy was kept sufficiently low to ensure survival of a portion of the precursor ion from each peptide species. Despite the relatively low collision energy used for the singly charged ions of interest, we were able to assign a number of the fragment ions in the individual MS/MS spectrum as well as observe the neutral loss of 98 Da from the single phosphopeptide in the mixture, as shown in Fig. 7.
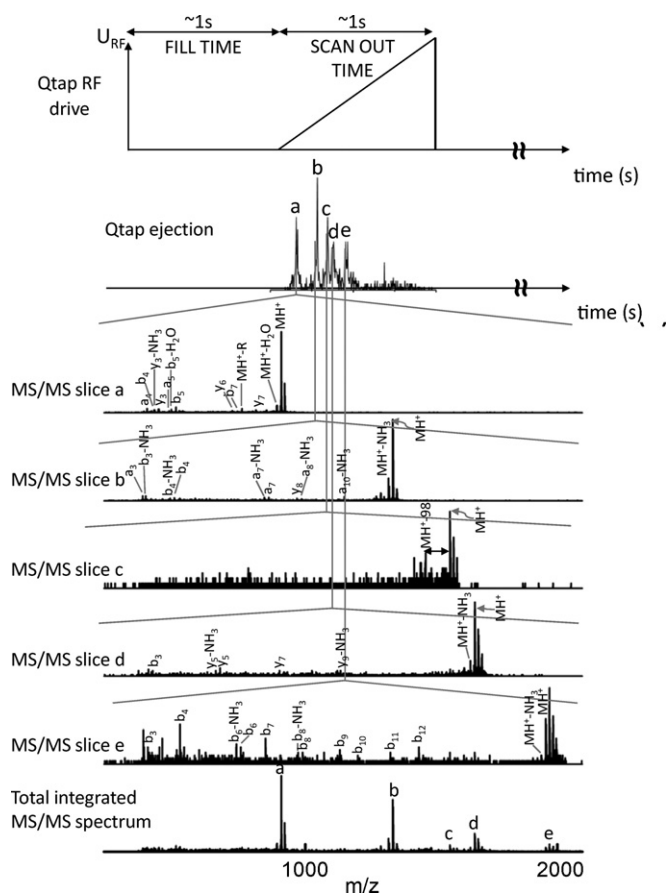
Fig. 7. (Top) MALDI ions from a 1-s fill and 1-s scan out shown in the Qtap ejection time dimension. The dataset was obtained from a 5 peptide mixture (500 fmol of each component). (Below) TOF MS/MS spectra obtained by integrating narrow regions about the gray solid lines (a–e) in the Qtap ejection time distribution. Fragments were generated by ramping the DC Bias on Qo (see Fig. 2b) from 40 to 100 V in sync with the Qtap ejection scan. (Bottom) Total integrated MS/MS spectrum from the entire dataset.

4. Discussion and conclusion

Here, we have demonstrated the feasibility of coupling a high-capacity ion trap (Qtap) to a TOF analyzer for comprehensive linked scans with no scanning losses. Our experiments show that we can obtain MS/MS information from all components in a mixture of peptides, and that it is feasible to extract multiple neutral loss information from a single experiment. Although the samples used in the present work are fairly simple, straightforward modifications of our current setup should allow us to study more complex samples. In our present study, two different variations of the instrument were tested – (I) Qtap-qTOF and (II) Qtap-qQqTOF. Based on the results shown, we have found that the extended configuration II is the better choice. There are two main reasons why this is the case: First, the additional quadrupoles (Q_o and Q_1 in Fig. 2b) decouple the Qtap from the collision cell and therefore sufficiently high pressures of argon can be used in the collision cell to induce collisional dissociation without significant argon contamination of the Qtap. Second, Q_o and Q_1 cool and focus the ejected ion beam prior to ion injection into the collision cell (Fig. 2b). Based on previous calculations, we estimate that ions are ejected with a considerable amount of kinetic energy from the Qtap (e.g., $\approx$100 eV for m/z 1673 ion [33]). By cooling the ions before the collision cell we minimize the ion losses to the rods from ions having too much kinetic energy. The extra quadrupoles also allow us to control the translational collisional energies of the ions as a function of m/z to elicit optimal collision induced dissociation.

Current limitations: While we have shown that our overall strategy works and have demonstrated that we can fragment all the ion species that are trapped in the Qtap, there are a number of factors that currently limit the performance of our prototype instruments. First, the overall ion transmission is low. In the compact configuration I, we lose a large portion of the ions in the source due to insufficient cooling of the MALDI ions as well as after ion ejection from the Qtap. This should be readily improved by incorporating an additional collisional cooling device in the source region and using additional collisional cooling post-ion ejection from the Qtap (as in the extended configuration II). In the ion source region, an additional ion guide can be incorporated to decouple the high-capacity ion trap from the source region, thus allowing us to use nitrogen to cool the MALDI-generated ions (as is now standard in commercial MALDI-QTOF and vMALDI-ion trap instruments). Another improvement can be made by going to a higher repetition rate orthogonal TOF analyzer, which produces a much higher number of spectra per second than we use in the present configuration. Currently there are benchtop TOF devices [44] that are able to produce spectra every 33 μs. This is approximately seven times faster than the 200 μs duration TOF spectra that we are currently using. Finally, we are using a relatively low acceleration potential (4 kV) in the TOF. Considerable improvement in ion detection and transmission can be achieved by increasing this acceleration potential. We estimate that by increasing the signal transmission with the additional cooling ion guides, increasing the TOF ion energy, and going to higher repetition rate TOF devices we should gain more than 2 orders of magnitude in signal.

Although, our prototype instruments use MALDI-generated ions, it should be straightforward to couple an electrospray ionization source to these devices, allowing the use of liquid chromatography for additional separation prior to MS and MS/MS analysis. Indeed, it should be straightforward to couple the ESI source at one entrance to the Qtap and MALDI at the opposite entrance, allowing for rapidly switchable ionization modes. The timescale of Qtap ion filling and subsequent ejection into the TOF analyzer is in the range 1–2 s, making it compatible with typical LC peak separation times of the order of a few to tens of seconds.

In summary, we have explored the properties of a novel prototype instrument that is capable of collecting MS/MS of all stored ion species with no prior mass selection. The significant advantage of this approach is that no prior knowledge of the sample is required before the experiment is performed because maximal information about the sample is collected, allowing comprehensive data analysis post-acquisition. This is achieved by sequentially ejecting all ions from a high-capacity ion trap (Qtap), collisionally fragmenting them upon ejection, and subsequently analyzing them by TOF MS. By recording TOF of all ions, we can acquire comprehensive MS/MS spectra of all fragment and precursor ions with high mass resolution and accuracy, after which the desired information can be extracted. This strategy will allow us to obtain comprehensive information from a particular sample in a single experiment, including accurate molecular masses, backbone fragmentation, the presence and location of posttranslational modifications, and particular fragmentation transitions that identify and quantitate particular peptides and peptide modifications – and hence advance the frontiers of proteomic research.

Acknowledgements

References

[1] F. Hillenkamp, M. Karas, R.C. Beavis, B.T. Chait, Anal. Chem. 63 (1991) 1193A.

[2] J.B. Fenn, M. Mann, C.K. Meng, S.F. Wong, C.M. Whitehouse, Science 246 (1989) 614.
[3] R. Aebersold, M. Mann, Nature 422 (2003) 198.
[4] I.V. Chernushevich, A.V. Loboda, B.A.J. Thomson, Mass Spectrom. 36 (2001) 849.
[5] J.V. Olsen, J.C. Schwartz, J. Griep-Raming, M.L. Nielsen, E. Damoc, E. Denisov, O. Lange, P. Remes, D. Taylor, M. Splendore, E.R. Wouters, M. Senko, A. Makarov, M. Mann, S. Horning, Mol. Cell. Proteomics 8 (2009) 2759.
[6] A. Schmidt, M. Claassen, R. Aebersold, Curr. Opin. Chem. Biol. 13 (2009) 510.
[7] C.L. Gatlin, J.K. Eng, S.T. Cross, J.C. Detter, J.R. Yates, Anal. Chem. 72 (2000) 757.
[8] D.L. Swaney, G.C. McAlister, J.J. Coon, Nat. Methods 5 (2008) 959.
[9] S.A. Carr, R.S. Annan, R.W. Kondrat, M.J. Huddleston, Methods Enzymol. 405 (2005) 82.
[10] D. Zakett, A.E. Schoen, R.W. Kondrat, R.G. Cooks, J. Am. Chem. Soc. 101 (1979) 6781.
[11] M.J. Cole, C.G. Enke, Anal. Chem. 63 (1991) 1032.
[12] M.J. Schroeder, J. Shabanowitz, J.C. Schwartz, D.F. Hunt, J.J. Coon, Anal. Chem. 76 (2004) 3590.
[13] H. Steen, M. Fernandez, S. Ghaffari, A. Pandey, M. Mann, Mol. Cell. Proteomics 2 (2003) 138.
[14] R. Niggeweg, T. Kocher, M. Gentzel, A. Buscaino, M. Taipale, A. Akhtar, M. Wilm, Proteomics 6 (2006) 41.
[15] R.H. Bateman, R. Carruthers, J.B. Hoyes, J. Jones, J.I. Langridge, I. Millar, J.P.C. Vissers, J. Am. Soc. Mass Spectrom. 13 (2002) 792.
[16] J.T. Stults, C.G. Enke, J.F. Holland, Anal. Chem. 55 (1983) 1323.
[17] S. Purvine, J.T. Eppel, E.C. Yi, D.R. Goodlett, Proteomics 3 (2003) 847.
[18] D.J. Kenny, J.M. Brown, M.E. Palmer, M.F. Snel, R.H. Bateman, J. Am. Soc. Mass Spectrom. 17 (2006) 60.
[19] A.A. Ramos, H. Yang, L.E. Rosen, X Yao, Anal. Chem. 78 (2006) 6391.
[20] J.D. Williams, M. Flanagan, L. Lopez, S. Fischer, L.A.D. Miller, J. Chromatogr. A 1020 (2003) 11.
[21] S.J. Geromanos, J.P.C. Vissers, J.C. Silva, C.A. Dorschel, G.Z. Li, M.V. Gorenstein, R.H. Bateman, J.I. Langridge, Proteomics 9 (2009) 1683.
[22] G.Z. Li, J.P.C. Vissers, J.C. Silva, D. Golick, M.V. Gorenstein, S.J. Geromanos, Proteomics 9 (2009) 1696.
[23] K. Blackburn, F. Mbeunkui, S.K. Mitra, T. Mentzel, M.B. Goshe, J. Proteome Res. 9 (2010) 3621.
[24] J. Wilson, R.W Vachet, Anal. Chem. 76 (2004) 7346.
[25] E.R. Williams, S.Y. Loh, F.W. McLafferty, R.B. Cody, Anal. Chem. 62 (1990) 698.
[26] C. Masselson, G.A. Anderson, R. Harkewicz, J.E. Bruce, L. Pasatolic, R.D. Smith, Anal. Chem. 72 (2000) 1918.
[27] L. Li, C.D. Masselson, G.A. Anderson, L. Pasa-Tolić, S.W. Lee, Y. Shen, R. Zhao, M.S. Lipton, T.P. Conards, N. Tolić, R.D. Smith, Anal. Chem. 73 (2001) 3312.
[28] C.S. Hoaglund, J. Li, D.E. Clemmer, Anal. Chem. 78 (2000) 2737.
[29] S.I. Merenbloom, S.L. Koeniger, S.J. Valentine, M.D. Plasencia, D.E. Clemmer, Anal. Chem. 78 (2006) 2802.
[30] S.J. Valentine, M.D. Plasencia, X. Liu, M. Krishnan, S. Naylor, H.R. Udseth, R.D. Smith, D.E. Clemmer, J. Proteome Res. 5 (2006) 2977.
[31] M.E. Belov, M.A. Buschbach, D.C. Prior, K. Tang, R.D Smith, Anal. Chem. 79 (2007) 2451.
[32] J.A. McLean, B.T. Ruotolo, K.J. Gillig, D.H. Russell, Int. J. Mass Spectrom. 240 (2005) 301.
[33] A.N. Krutchinsky, H. Cohen, B.T. Chait, Int. J. Mass Spectrom. 268 (2007) 93.
[34] A.N. Krutchinsky, M. Kalkum, B.T Chait, Anal. Chem. 73 (2001) 5066.
[35] T.W. Jaskolla, W.D. Lehmann, M. Karas, Proc. Natl. Acad. Sci. U.S.A. 105 (2008) 12200.
[36] A.N. Krutchinsky, W. Zhang, B.T. Chait, J. Am. Soc. Mass Spectrom. 6 (2000) 493.
[37] E.B. McCauley, US Patent 6,593,569, February 8, 2001.
[38] I.V. Chernushevich, A.V. Loboda, B.A. Thomson, J. Mass Spectrom. 36 (2001) 849.
[39] A. Loboda, A. Krutchinsky, O. Loboda, J. McNabb, V. Spicer, W. Ens, K. Standing, 48th ASMS Conference on Mass Spectrometry and Allied Topics, June 11–15, Long Beach, CA, 2000.
[40] R.S. Annan, S.A. Carr, Anal. Chem. 65 (1993) 1021.
[41] J. Qin, B.T. Chait, Anal. Chem. 69 (1997) 4002.
[42] S.A. McLuckey, C.L. Glish, K.G. Asano, Anal. Chim. Acta 225 (1989) 25.
[43] I. Haller, U.A. Mirza, B.T. Chait, J. Am. Soc. Mass Spectrom. 7 (1996) 677.
[44] Waters Xevo QTOF Mass Spectrometer.